Building and Environment 245 (2023) 110904

Contents lists available at ScienceDirect

Building and Environment

journal homepage: www.elsevier.com/locate/buildenv

Porous plant form-induced amplification of evapotranspiration for enhanced cooling in vertical greenery systems

Iqbal Shah [a], Siu-Kit Lau [b], Veera Sekaran [c], Ali Ghahramani [a,*]

[a] *Department of the Built Environment, College of Design and Engineering, National University of Singapore, Singapore*
[b] *Department of Architecture, College of Design and Engineering, National University of Singapore, Singapore*
[c] *Department of Biological Sciences, Faculty of Science, National University of Singapore, Singapore*

ARTICLE INFO

Keywords:
Urban greening
Urban heat island
Living wall
Façade thermal performance
Energy savings
Green wall

ABSTRACT

Vertical Greenery Systems (VGS) installed on building façades have recently gained significant attention for its urban cooling potentials. While current research primarily leans on the Leaf Area Index to estimate the VGS cooling potentials, the evaporative cooling effects of VGS growing media, has largely been overlooked. In particular, the effect of plant growth form on air movement within the VGS, which could notably augment the rate of evapotranspiration, has commonly been ignored. To address this gap, our study undertakes a comprehensive thermal analysis of two distinct plant growth forms (porous and dense), combining systematic Computational Fluid Dynamics simulations with field experiments over a six-month period. Our results, for the first time, demonstrate that the provision of a porous VGS significantly enhances its cooling effects, which could even lead to a negative façade heat flux. Our findings offer a novel perspective for plant and growing media selection in VGS design.

1. Introduction

Representing approximately 40 % of global energy consumption and greenhouse gas emissions, buildings have a significant impact on environmental sustainability [1]. In particular, energy utilized for building cooling systems is estimated to make up about 20 % of global total, and a notable 56 % in tropical regions [1,2]. As global warming trends project an increase in ambient air temperature by 0.4 °C–0.6 °C each decade [3], the strain on building cooling systems is poised to intensify. With every 1 °C increase in outdoor air temperatures potentially triggering an 8.5 % surge in cooling energy consumption [4], a considerable 12.75 % rise in cooling loads over the next three decades is expected. Additionally, densely urbanized areas often experience the Urban Heat Island (UHI) effect, which leads to an average temperature increase of 3 °C, consequently amplifying cooling consumption by about 25 % [5]. The UHI effect, exacerbated by global warming-induced rises in ambient air temperatures, perpetuates a vicious cycle of increasing anthropogenic heat [6,7]. These trends underscore the urgent call for an effective sustainable strategy to decrease cooling energy demands for the urban built environment, while simultaneously alleviating the UHI effects.

An increasingly recognized strategy for mitigating the effects of UHI and reducing heat absorption through building facades involves the use of Vertical Greenery Systems (VGS) [8]. Utilizing their unique vertical structure of plant cover, VGS offer a myriad of direct and indirect cooling effects (refer to Fig. 1.), making them an increasingly popular solution in urban design [9,10]. Researchers commonly utilize the Leaf Area Index (LAI) as the primary metric for assessing the cooling potentials of VGS—predicated on the belief that a greater LAI generally leads to enhanced leaf shading and evapotranspiration. However, relying solely on LAI neglects other significant factors such as the multifaceted nature of plant growth forms, the role of the growing medium, and the impact of seasonal and diurnal changes on VGS cooling. For instance, LAI fails to account for 'midday stomatal closure' [11], where plants close their stomata during the hottest parts of the day, thereby inadvertently reducing evapotranspiration and its cooling effect when it's most needed. As depicted in Fig. 1., the true cooling potentials of VGS emerge from a complex interplay of multiple heat transfer mechanisms, underscoring the importance of considering all components in the cooling process.

One of the key components in this context is the evaporative cooling from the VGS growing media, which assists in cooling the building and the surrounding environment through convective heat transfer. While previous studies have highlighted that ambient wind and local vortices due to convective heat transfers can stimulate air movement within

* Corresponding author.
E-mail address: ghahramani@nus.edu.sg (A. Ghahramani).

https://doi.org/10.1016/j.buildenv.2023.110904
Received 1 August 2023; Received in revised form 1 October 2023; Accepted 4 October 2023
Available online 11 October 2023

terrestrial vegetation and intensify the rate of evaporation from the ground surface soil [12–14], no study has yet examined the impact of plant form porosity on air movement and the resulting cooling effects within the VGS.

Therefore, our study seeks to investigate the impact of the plant form porosity on the air movement, cooling effect, and thermal performance of VGS. We specifically contrast plant species exhibiting distinct growth forms, one which creates larger air gaps (porous growth form) between the leaf layer and growing media, against species that forms limited air gaps (dense growth form). The hypothesis being tested is that growth forms leading to larger air gaps (porous) would correspondingly yield a higher VGS cooling effect (Refer to Fig. 1). Thus, this study undertakes a comprehensive analysis of VGS thermal performance, by selecting two distinct species of epiphytic plants—each exemplifying a dense and a porous growth form respectively. Our approach combines systematic Computational Fluid Dynamics (CFD) simulations with long-term field experiments conducted in two phases, six months apart. We have two main objectives: (1) to quantify the potential enhancement in VGS cooling effects offered by larger air gaps between the VGS leaf layer and growing media (VGS porosity), and (2) to assess the significance of different plant growth forms on the overall VGS thermal performance, specifically focusing on the façade heat gain reduction and outdoor cooling effects.

The comprehensive findings of this study offer a novel perspective in the selection of plant species and growing media for VGS design, by emphasising considerations for promoting airflow between the leaf layer and growing media. This approach has the potential to optimize the cooling effects of VGS especially during the warmest parts of the day. Given the diverse benefits of VGS, which include enhancing mental wellbeing, promoting social cohesion, and fostering urban biodiversity, a carefully designed VGS can significantly contribute to the creation of an urban built environment that is more energy-efficient, sustainable, biodiverse, and liveable.

The structure of this paper is as follows. Section 2 provides a literature review of the factors affecting VGS thermal performance, as well as recent studies on the types of VGS systems currently available. Section 3

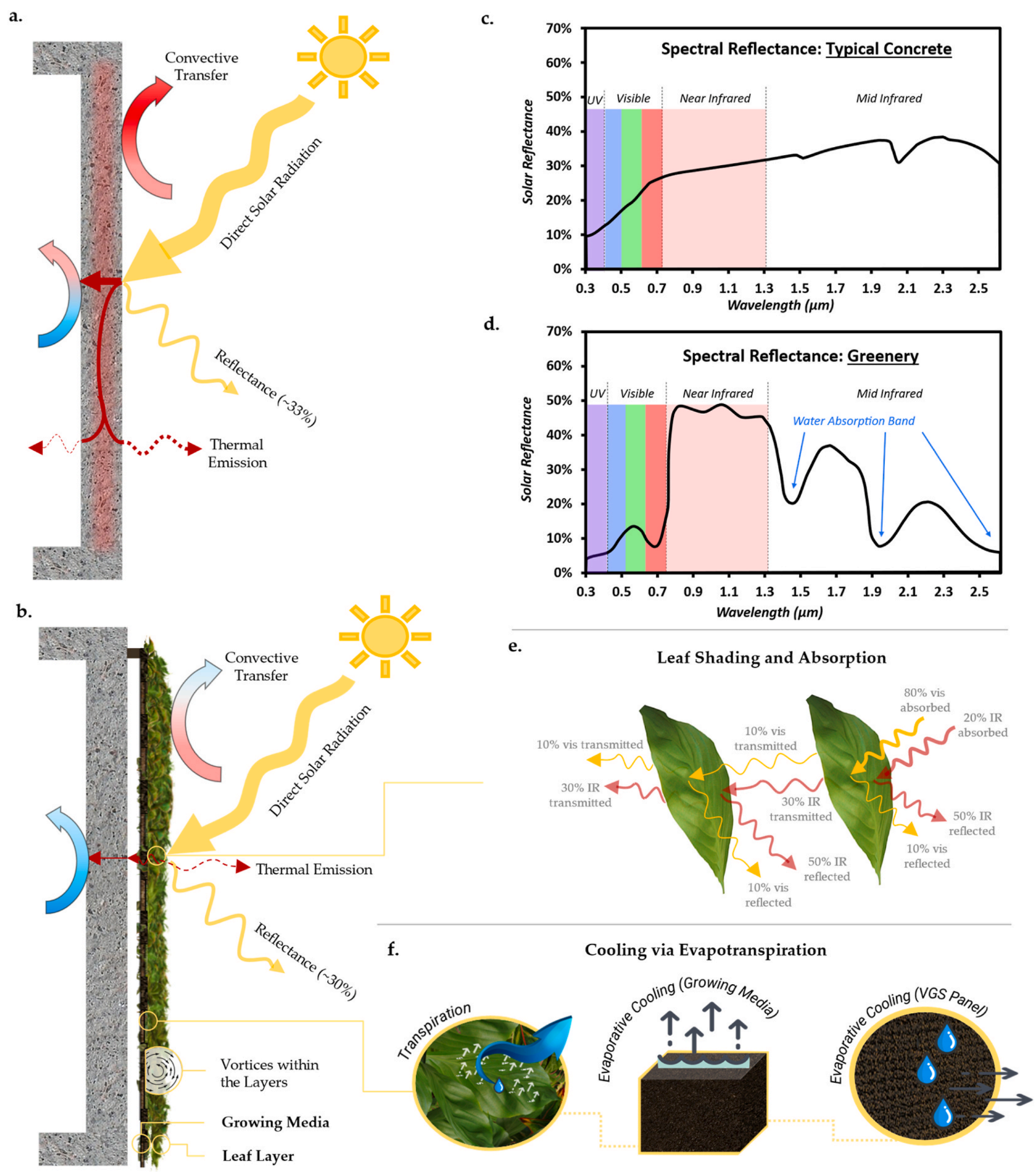

Fig. 1. Conventional Façade vs Vertical Greenery System (VGS) Façade Thermal Balance Mechanisms. (a) Thermal Balance for Conventional Façade. **(b)** Thermal Balance for VGS façade. **(c)** Spectral Reflectance of Conventional Façade. **(d)** Spectral Reflectance of VGS Façade. **(e)** VGS Leaf Shading and Transmissions. **(f)** VGS Cooling Mechanisms.

explains the methodical approach of data collection and analysis for the CFD, and experiments conducted in this paper. The results of the experiments would then be presented in Section 4. Subsequently, Section 5 presents a discussion of the CFD and experimental results, along with the limitations and potential for work for future studies. Section 6 would then summarise the key findings and concludes the paper.

2. Literature review

This literature review undertakes a meticulous exploration of VGS, focusing first on the pivotal elements influencing their thermal performance. These elements include plant species selection, shading and growth coverage of VGS, along with the consideration of the VGS growing media and panel construction material. Each of these factors significantly influences the modulation of the VGS thermal characteristics [15]. This paper allocates close attention to the potential impact of these variables on VGS cooling performance, particularly when plant form porosity is induced - a central hypothesis of our investigation. Further, we delve into the array of VGS classifications, aiming to discern those systems that could potentially reap the most benefits from the induction of VGS plant form porosity. The introduction of such elements has profound implications on outdoor convection and the production of micro vortices within the VGS [14]. These convection and micro vortices could potentially enhance the VGS outdoor cooling effects and augment the VGS conductive insulation properties, thus shaping the overall thermal efficiency of the system. Our objective through this multi-faceted review is to deliver a comprehensive understanding of the complex interplay between these various factors and their consequential impact on the thermal performance of VGS.

2.1. Factors affecting VGS thermal performance

The complex processes that drive the cooling effects of vertical greenery systems (VGS) are multifaceted. These key mechanisms, though intricate, have been broken down and visually presented in Fig. 1. Fig. 1(a) showcases the heat transfer mechanism at play in a typical bare concrete façade. This involves conductive heat gain and heat storage, facilitated by the thermal mass of the concrete, as well as convective heat transfer both inside and outside [16]. The latter is due to the heat exchange between the ambient air/wind with the hot/warm surface temperature of the exposed façade. Additionally, the concrete's thermal mass absorbs and stores heat, which is then emitted as radiation to the environment, affecting both indoor and outdoor surroundings. In contrast, Fig. 1(b) illustrates the heat transfer mechanism of a typical living wall-type VGS. It's interesting to note that the spectral reflectance of the VGS closely matches that of the concrete façade, as shown in Fig. 1 (c). However, the significant dips in spectral reflectance visible in Fig. 1 (d) are in fact the water absorption bands of the greenery [17,18]. Moreover, Fig. 1(e) reveals how the multiple layers of leaves and panel shading shades the actual building structure from direct solar radiation, reducing the transmission of radiation by approximately 5–10 % within each layer [19]. This transmission becomes potentially much lower as it reaches the VGS panel. Fig. 1(f) goes on to detail the cooling mechanisms within the VGS that contribute to its cooling effect. Specifically, the water absorption bands within the solar radiation spectrum, coupled with heat from the surroundings, are being utilized in a process known as latent heat of vaporization (resultant is also known as the process of evapotranspiration). This process helps to keep the surfaces of the VGS significantly cooler than a traditional concrete façade. However, it is important to note that the magnitude of cooling effect produced by the VGS is largely dependent on key factors such as (1) plant species utilized, (2) VGS shading and growth coverage, as well as (3) VGS growing media and construction material.

2.1.1. VGS plant species

The rich diversity of plant species presents an extensive selection palette for integration into VGSs. However, the key aspect to weigh in this selection process is not just the variety but the resilience of the plants. The survivability/sustainability of the chosen plant species is central to the enduring functionality and cooling effectiveness of the VGS. In essence, even if a plant species possesses exceptional thermoregulatory properties, its utility could be significantly diminished if it cannot endure over a prolonged period within the VGS environment. Among the spectrum of resilient plants, epiphytic species emerge as a particularly promising group. Epiphytes, by nature, have a remarkable ability to adapt to varied conditions. This is an attribute supported by Ref. [20] who suggest that most epiphytic plants exhibit clonal growth habits that increases the chances of its survivability. Epiphytic plants are defined by their symbiotic existence, latching onto other plants, substrates, or surfaces. They act as biological sponges, absorbing nutrients and moisture from their immediate environment [21]. This biological adaptation allows them to endure harsh conditions, such as nutrient deficiencies and water stress. This innate resilience and versatility further bolster their appeal as potential components within VGS. The potentials of epiphytic plants extend beyond their ability to anchor themselves to other plants or surfaces. They can also be cultivated in soil substrates as ornamental additions [20,22], thereby broadening their applicability within a VGS setting. Physiologically, epiphytic plants often possess a high density of trichomes, which facilitate absorption of nutrients from the ambient air and surrounding areas [21]. This unique capability implies a higher rate of evapotranspiration and thus, a stronger cooling effect – a desirable characteristic in the context of VGS. Given these considerations, the selection of epiphytic plant species for this study is well-grounded. Their inherent adaptability, resilience, and cooling potential, coupled with their ability to thrive in the porous and dense growth environments required for VGS, make them an attractive option.

2.1.2. VGS shading and growth coverage

The Leaf Area Index (LAI), a ratio calculated by dividing a plant's total leaf area by its ground coverage, serves as a commonly used metric for assessing the shading and growth coverage of VGS. Notably, the importance of VGS plant growth coverage extends beyond the shading effects that it provides. In fact, it also has an impact on, solar absorption within the VGS construction material, rate of evapotranspiration (augmented by the number of leaves), and VGS albedo. This is reinforced by Ref. [23] who suggest that there is a strong positive relationship between LAI and a decrease in soil and air temperature within the VGS layers. In addition, a simulation study by Ref. [24] also found that the increase in LAI value of a VGS from 1 to 5 would result in a 12 °C reduction to exterior wall surface temperature. This is a significant reduction that reveals the potentials of VGS in mitigating the effects of UHI. However, since the Leaf Area Index (LAI) does not consider the porosity of the plant growth form in the VGS, it is vital to acknowledge that past studies on VGS growth coverage may have overlooked the potential influence of plant form porosity variations on the thermal performance of their VGS. Additionally, is essential to note that the current process of obtaining LAI values of a VGS would take an extensive amount of time and effort, yet the computations would not be exactly as the plants continues to shed and grow new leaves [25]. Therefore, some studies such as [26] utilize a simplified approach where the paper only provided an indicative value of substrate and plant thickness when comparing between the different VGS being tested.

2.1.3. VGS growing media and panel construction material

The growing media of a VGS is an essential component that positively affects the evaporative cooling potential of a VGS. A recent study by Ref. [27] conducted in-depth comparison of 16 different growing media composition on a VGS to identify its effects on thermal insulation. The study found that the growing media composition that consist of coco-peat provided superior thermal insulative characteristics. This was due to the fact that peat has a superior water holding characteristic, which allows it to hold and slowly release the cool irrigation water throughout the day, forming an insulative barrier. Besides contributing towards the evaporative cooling effect, the growing media in a living wall system could also acts as an insulative barrier that reduces the conductive heat gain through a façade. Therefore, it is also essential to place due consideration for the growing media composition of a VGS.

Besides the consideration for VGS soil substrate, the material utilized in a VGS construction especially for Living wall system also has a significant impact on VGS thermal insulation [27]. Typically, the VGS modular tray or pots are constructed with Polypropylene (PP), or High-Density Polyethylene (HDPE), whereas the pocket or flexible bag and lightweight panels are typically constructed out of Polyethylene Terephthalate (PET) felt. Selection of a more breathable and water absorptive VGS construction material could also potentially yield higher levels of evaporative cooling effects especially when a porous plant growth form is utilized on the facade.

2.2. Types of VGS classification

An array of terminologies exists within the literature on Vertical Greenery Systems (VGS), making it crucial first to decipher the different classifications. As noted by Ref. [28], VGS refers to processes for vertical plant cultivation, interchangeably termed as green walls, vertical gardens, and vertical landscapes [29]. Fig. 2 succinctly illustrates the classifications, revealing 12 subtypes categorized by Growing Media, Construction and Installation Methodology, and Plant Types. The various VGS systems available presents an assortment of options for urban greenery implementation. These systems can generally be categorized into two primary types - Green Façade (GF) and Living Wall (LW) [30,31]. This bifurcation primarily stems from the different mediums used for plant growth in each system. In GF systems, the growth medium is strategically positioned either at the base or on a ledge system, facilitating upward growth or downward hanging of foliage, typically climbers or hanging plants. LW systems on the other hand, offer individual carriers or panels with multiple pockets, which house both the growth medium and the plant. These are then affixed to the wall. Notably, LW systems offer a more expansive range of plant species and provide greater ease of maintenance compared to GF systems [29].

Further refinement of these classifications has been introduced by Ref. [32], taking into consideration the specific construction characteristics employed in VGS deployment. For example, in a direct GF system, plants are directly affixed to the vertical surface, while an indirect GF system employs a support structure, such as a steel mesh, to encourage plant growth. The Continuous Guide and Modular Trellis methods differ by the extent of their supporting structure. A continuous guide uses a single structure to facilitate plant growth across its entire surface, while a modular trellis utilizes several modular structures installed on the vertical surface. Both methods cater to climbing plants and those that hang downwards [32]. also classified LW systems into Continuous and Modular types. The Continuous system employs permeable, lightweight screens or panels, into which plants are individually inserted to grow. The Modular LW system, on the other hand, incorporates the use of trays, planter boxes, planter tiles, vessels, and flexible bags to cater to a wide array of applications.

Besides classification based on growing media and construction/installation method, in an early study by Ref. [33], VGS were instead classified by plant types. The study classified VGS into four categories, namely Tree-against-wall, Hanging-down type, Wall-climbing type, and Module-type [33]. The plants employed by each of those classifications are Trees, creeping plants, plants with long stems hanging down, as well as the typical potted plants respectively. It is essential to also note at this stage that there are currently still no studies that classifies plants on VGS based on their growth forms (porous and dense) which is therefore the central area of investigation in this study.

3. Methods

A study employing Computational Fluid Dynamics (CFD) simulation

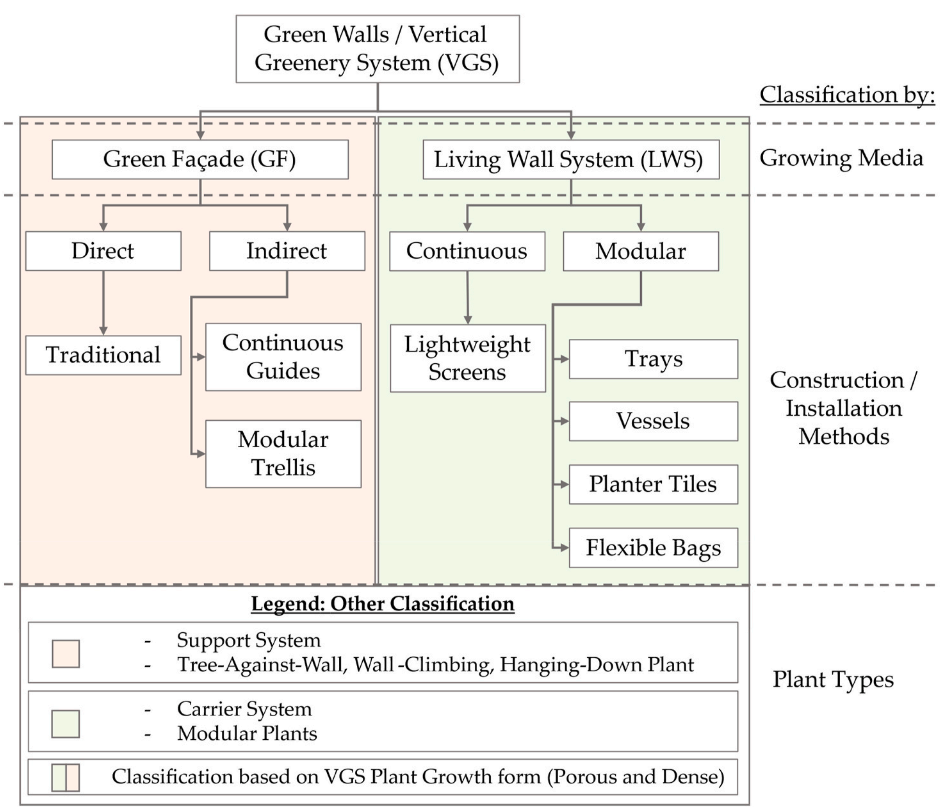

Fig. 2. comprehensive illustration of VGS systems and classifications.

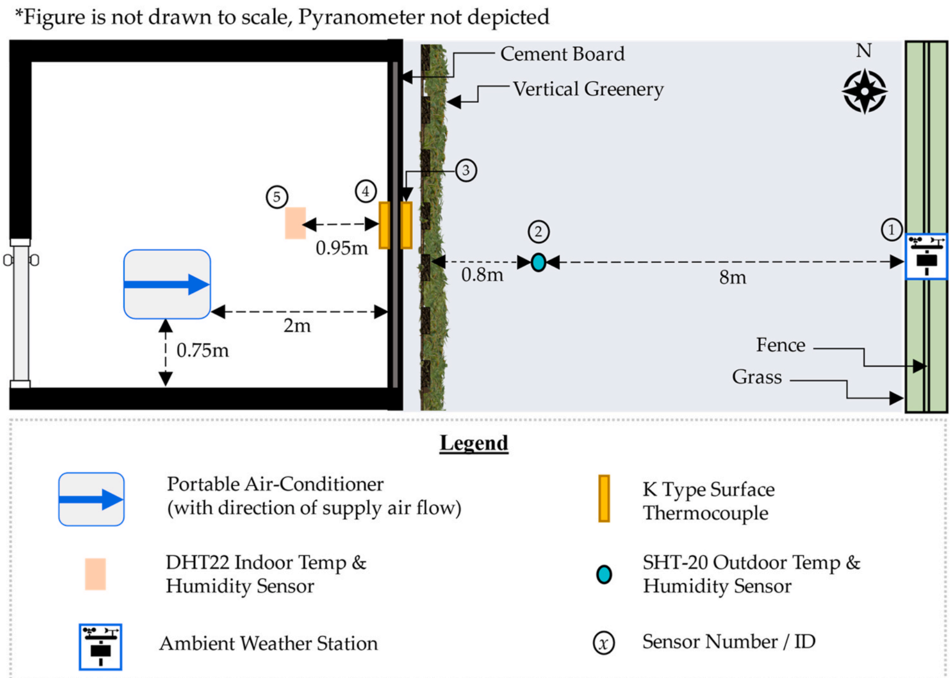

Fig. 3. | VGS thermal performance experiment layout.

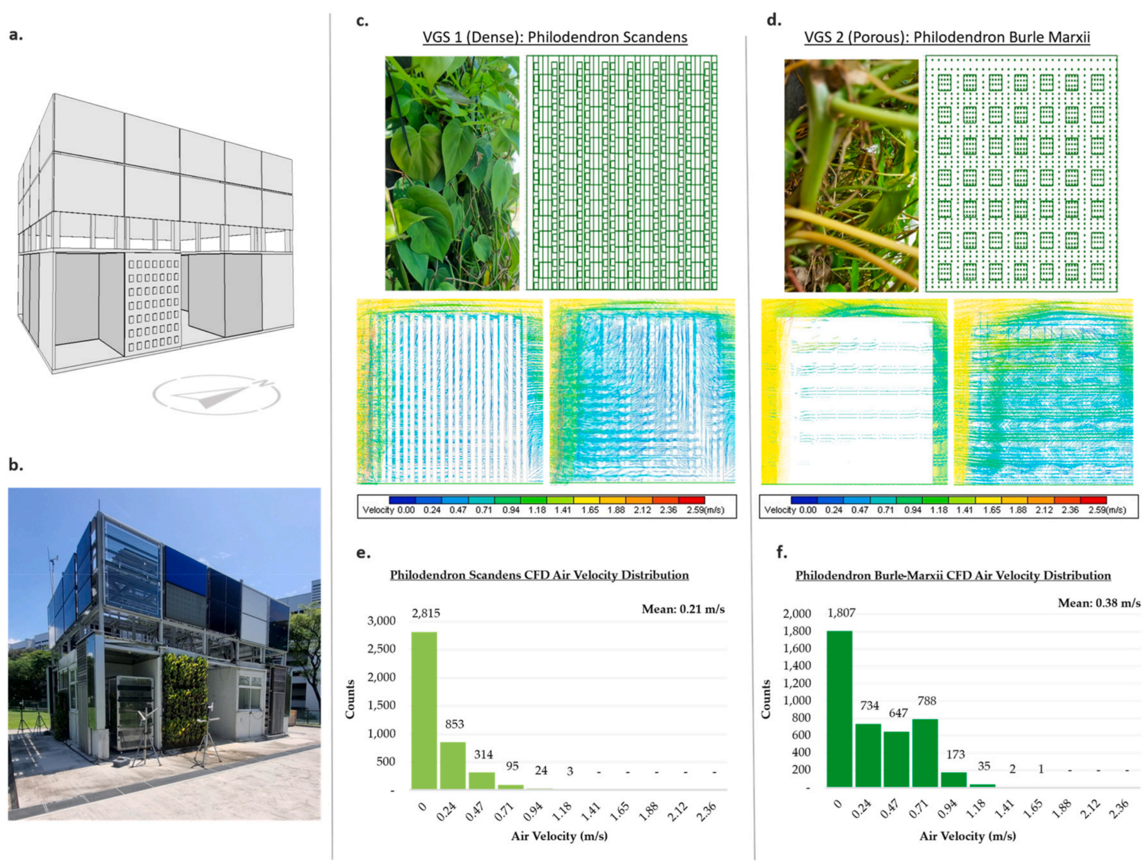

Fig. 4. CFD of air flow through two different plant types/growth form. a, DesignBuilder Model of the Tropical Technologies Laboratory. **b**, Real-world illustration of setup at the Tropical Technologies Laboratory. **c**, Cross-section of VGS 1(dense) growth form (Top left), CFD model grids of VGS 1 (Top right), air flow patterns through VGS 1 with visible component block (bottom left), air flow pattern through VGS 1 without component blocks visible (bottom right). **d**, Cross-section of VGS 2 growth form (Top left), CFD model grids of VGS 2 (Top right), air flow patterns through VGS 2 with visible component block (bottom left), air flow pattern through VGS 2 without component blocks visible (bottom right). **e**, Graph velocity count for VGS 1 based on the patterns of the air flow. **f**, Graph velocity count for VGS 2 based on the patterns of the air flow.

was initially undertaken to investigate the potential enhancement of evaporative cooling resulting from a porous plant growth structure within a Vertical Greenery System (VGS). The study specifically examined how introducing an air gap between the leaf layer and growing medium could influence wind speeds, and consequently, the associated potential for evaporative cooling from the growing medium. Following this, a practical experiment mirroring the layout of the CFD study was implemented to contrast the thermal performance of porous and dense VGS plant growth at two distinct growth stages separated by six months. This real-world experiment allowed us to validate the outcomes of the CFD simulation, with soil moisture levels measured to understand the evaporation rate, and the associated impacts on the VGS thermal performance (both heat gain reduction and outdoor cooling effects).

3.1. CFD simulation parameters

A 1.7 m by 2.6 m East facing façade was first modelled after the laboratory available for thermal performance experiments in the real world. Component blocks were then used to manually create the simplified structure of the two different VGS as illustrated in Fig. 4 (c) and (d). Component blocks in DesignBuilder are essentially elements that does not contain zones, typically used for modelling structures of shading devices. The VGS panel was the modelled consisting of a grid of 7 by 7 pocket spaced evenly on the full wall VGS panel, with each pocket being 200 mm by 200 mm with a 45 mm protrusion. The model of the dense VGS utilizes 21 full height panels with a width of 80 mm to illustrate the upward creeping or downwards hanging for of dense VGS plants. There are also alternating patterns of 19 ridges which are of 45 mm depth and 80 mm height, spaced equally at the back (extends towards and touching the VGS panel) of each of the 21 full height panels, illustrating the overlapping nature of these plants. The porous VGS was instead modelled with 1871 protruding stems (perpendicular to the VGS panels) which are 10 mm by 10 mm by 100 mm protrusion from the VGS panel and 35 mm protrusion from stems that came from the pockets. At the outer end of the stem is a uniform full coverage panel to illustrate the single layer of uniform coverage from such porous growth form. The default site domain factor (values that are added from the sides and top of the model) of 3 m, 3 m and 2 m for the length, width and height were applied to specify the boundary of the model.

The external CFD parameter settings were configured as follows: The grid type was set to non-uniform, with the grid generated based on key model features. The default grid spacing, and grid line merge tolerance was set at 0.05 m, resulting in a total cell count of 1,225,440. This count is comprised of 115, 96, and 111 cells in the X, Y, and Z dimensions respectively. Additionally, the maximum grid aspect ratio obtained was 6.042. By default, DesignBuilder uses the Finite Difference Method (FDM) for its discretization scheme. The upwind scheme is incorporated to address the convection term within the fluid flow equations. Furthermore, the Semi-Implicit Method for Pressure-Linked Equations (SIMPLE) algorithm serves as the default mechanism for pressure-velocity coupling.

The wind velocity was set at 2.65 m/s in accordance with Singapore's mean wind velocity [34]. Wind direction was set to 180° corresponding to one of the predominant directions of wind in Singapore which is flowing towards North. The velocity set in DesignBuilder is the free stream wind velocity which is essentially the velocity at 10 m above ground level. The uniform free stream wind velocity was selected as this simplified CFD was designed as an initial study to understand the approximate magnitude of wind that is flowing through a VGS. In addition, the wall thermal properties, fluttering movements of leaves, and moisture transport with its interactions with the air are not taken into account in the CFD simulation for wind flow through the simplified VGS model. Rather, the simulation we have conducted was the first preliminary study to investigate the impact of plant form porosity on the approximate magnitude of wind that flows through the system.

The settings for turbulence model were set to K-epsilon turbulence model, which is the most widely used model belonging to the Reynolds Average Navier-Stokes group of models, where the turbulence kinetic energy and its dissipation rate of the turbulence kinetic energy was accounted for. The simulation was run until the normalized residuals for mass, X-velocity, Y-velocity, and Z-velocity converged at 0.0001. This convergence was achieved after 14,000 iterations.

Validation of the CFD results was done on the fully developed VGS (after 6 months of growth) by measuring the soil moisture level of the 2 VGS at 2pm (2 h after its previous irrigation watering). The soil moisture measurements were taken using the Grove capacitive soil moisture sensor which has an accuracy of ±5 % from each pocket within the VGS, the day before its thermal performance test was conducted. The data obtained is then processed using python's matplotlib pyplot to produce a quadratic interpolated heatmap for visualizing the distribution of soil moisture level for visual comparison with the CFD rendering. In addition, a comparison of mean with the calculated rate of evaporation from the soil, based on the CFD simulation results was also conducted. The equation for the rate of evaporation on the surface [35] is shown in *Equation (1)* and *Equation (2)* below. Subsequently the potential evaporative cooling effect could then be calculated using *Equation (3)*.

$$E_s = E_c \text{ x } (A) \text{ x } (X_s - X) \qquad \text{Equation (1)}$$

$$E_s = (25 + 19v)\ x\ (A)\ x\ (X_s - X) \qquad \text{Equation (2)}$$

$$Q_e = L\ x\ E_s \qquad \text{Equation (3)}$$

E_s:Rate of evaporation (kg/m^2/hour)
E_c:Evaporation Coefficient (kg/m^{2}h)
v:Velocity of air above the surface of the water (inputs from CFD, m/s)
A:Water surface area (1 m^2)
X_s:Maximum humidity ratio of saturated air (0.027125 kg/kg for the study's location)
X:Humidity ratio of air at existing state (0.171159 kg/kg)
Q_e:Evaporative Cooling (kJ/m^2/hour)
L:Latent heat of vaporization for water (2260 kJ/kg)

3.2. Experimental setup (VGS design considerations)

A set of VGS design considerations was established to serve as the fundamental components of the simulations and experiments conducted in this study. The key elements underpinning this consideration include (1) plant species, (2) VGS panel and growing media, and (3) area of leaf coverage (sampling stages) which were found in the literature review to be the key factors affecting VGS cooling potentials for this study.

3.2.1. Plant species selection

Beyond the porosity of plants' growth form, a central hypothesis of this study, another key consideration is the resilience of plants in a VGS. Despite excellent cooling properties, a low survival rate could substantially compromise the long-term cooling efficiency of the VGS. Given the proven adaptability of epiphytes to survive in varying weather conditions [20,36], we have selected two species of epiphytic plants for this study: Philodendron Scandens (VGS 1), exemplifying a dense growth form (climbing herbaceous vines), and Philodendron Burle-Marxii (VGS 2), representing a porous growth form (herbaceous, low-growing shrub) providing thick uniform coverage with an air-gap behind the leaves. Epiphytic plants have the added advantage of possessing more trichomes, which enables them to absorb the essential nutrients from the ambient air and surrounding areas [21,22]. This characteristic implies a potentially higher rate of evapotranspiration, hence enhancing the cooling effect. Fig. 5(a) illustrates the comprehensive VGS setup, while Fig. 4(c)(d) provides a cross-sectional view of both VGS types. These models in Fig. 4(c)(d) depicts a simplified representation of both VGS 1 and 2.

a.

VGS Specifications	VGS 1a	VGS 1b	VGS 2a	VGS 2b
Visual Estimate of VGS Coverage (%)	90	100	60	100
Thickness of Plant layer (mm)	50	100	80	120
Thickness of Substrate Panel (mm)	50 (including Pockets with soil), 20 (Panel only)			

b.

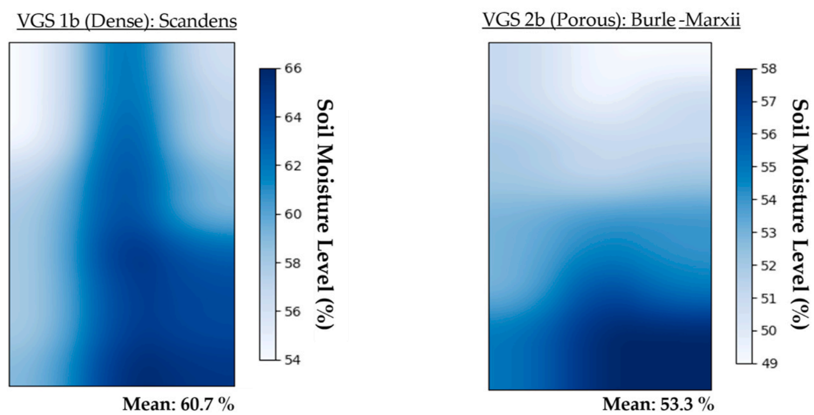

Fig. 5. VGS Characteristics and Layout for Experiment. a, dimensions, and growth description of the VGS tested. **b,** Site layout illustrating position of VGS, sensors and equipment. **c,** VGS 1b and 2b panel soil moisture percentage and distribution.

3.2.2. *VGS panel and growing media selection*

In the experiment, we utilized GVG substrate panels, a lightweight variant of the Living Wall System. These panels were selected based on their rated ability to hold up to 6 L of water per square meter, a quality that intensifies the potential for augmented evaporative cooling effects. These effects are particularly amplified with increased air movement from the airspace between the leaf layer and growing media. Paired with these panels, the growing media (an equal mix of coco peat and general compost) furthers the potential for cooling. This blend not only promotes balanced water absorption, augmenting evaporative cooling effects, but the general compost component also improves aeration essential for root breathability and serves as a nutrient source for plant growth [27,37].

3.2.3. *Area of leaf coverage (sampling stages)*

Leaf coverage is a factor that holds importance since it may significantly affect the rate of evaporation from the growing media. This is primarily due to the decrease in incident solar radiation on the growing media, a consequence of leaf-induced shading [19,24]. To evaluate this potential impact, our study conducted experiments at two distinct phases of leaf coverage. The initial phase corresponds to the transplanted state of the VGS onto the system, denoted as VGS 1a-Dense and VGS 2a-Porous. The subsequent phase captures a state where leaf coverage is at its maximum (100 %), denoted as VGS 1b-Dense and VGS 2b-Porous. By doing so, we aim to assess how leaf coverage might influence the cooling performance of both dense and porous VGS at different stages of operational and maintenance cycles. Corresponding values for leaf coverage are presented in Fig. 5(a).

3.3. *Site preparation and thermal performance measurements*

The experiment was conducted on an east-facing opaque façade. To obtain realistic results, the façade is constructed of a fibre-reinforced cement board with a thermal conductance value 4.004577 W/m^2K (Envelope thermal transfer value of 48.05 W/m^2). The deployment of sensors and VGS has been illustrated in Fig. 3. The accuracy of all temperature sensors in this experiment is ± 2 °C, and the air-conditioning energy monitoring using the Kasa KP115 smart plug may yield an error of up to 4 % in Watts. The pyranometer utilized is the Kipp & Zonen SMP10 which is within the Class A specifications of ISO 9060.

All sensors available were logged at a per second interval, with the exception of the pyranometer and weather station which captures data every minute and is logged based on an aggregated 5-min interval. The room depicted in Fig. 3 measures approximately 2.7 by 1.7 m, whereas the east-facing façade is approximately 1.7 m by 2.6 m high. The dual hose portable air-conditioning for the room was set at 24 °C throughout the measurement period. The full experimental setup can be found in Fig. 3 below.

There are 3 iterations that was tested at 2 different periods (initial state and 6 months later), (1) Baseline wall (no VGS), (2) VGS 1: Philodendron Scandens, and (3) VGS 2: Philodendron Burle-Marxii. The experimental duration to test each iteration was between 72 and 120 h, well within the minimally 72 h recommended in both [38] as well as ISO 9869-1 (2014) [39] for the heat flux measurement and calculations. The method of heat flux estimation using surface thermocouples has also been conducted in previous studies [38,40]. *Equation (4)* below shows the formula for computing the heat flux.

$$q = C(T_{es} - T_{is}) \qquad \text{Equation (4)}$$

q:heat flux through facade (W/m^2)
C:Thermal conductance value of the fibre reinforced cement board ($4.004577\ W/m^2K$)
T_{es}:External wall surface temperature
T_{is}:Internal wall surface temperature

3.4. Data analysis for VGS thermal performance

The dataset, logged at per-second intervals, was first processed using a Rolling Median filter, which helped to lessen the influence of outliers. This dataset was then converted into hourly and 5-min intervals respectively, wherein the average value was computed for each interval. This enhances the clarity for further analysing and presenting the findings. Besides looking at a the 24-h data, a daytime (8am to 8pm) truncated data was also generated to better understand the performance of VGS during the period of peak solar radiation exposure.

An independent *t*-test is then conducted to compare the significance between two data set. The Shapiro-Wilk test for normality is first conducted, of which if the p-value is more than 0.05, the dataset is normal, and therefore the student's t-test would be utilized, and if the dataset is less is not normal ($p < 0.05$), Mann-Whitney test would be utilized.

In addition, a regression and correlation analysis were also conducted to normalize the conductive heat gain and outdoor air temperature 800 mm away from the façade, against the varying weather conditions. This normalization allows for a standardized comparison among different iterations tested, effectively neutralizing varying weather conditions as a potentially confounding variable. For the regression and correlational analysis, a check for normality would first be conducted using Shapiro-Wilk's Test. If the distribution of the dataset is found to have a p-value of less than 0.05 based on the Shapiro-Wilk's test for normality, Kendall's tau-b correlation coefficient would be used for the correlational analysis. However, if the p-value in the test for normality is found to be more than 0.05, Pearson's r correlation coefficient would instead be used for the correlational analysis. The regression analysis was specifically applied to the 8am to 8pm (daytime) dataset to delve deeper into the impact of weather conditions on key factors, such as heat flux and outdoor temperatures in proximity to the VGS, throughout the day.

4. Results

4.1. CFD-based evaluation of air movement in different plant growth forms

Incorporating key factors discussed in the previous sections, such as the plant growth form, VGS panel and growing media characteristics, as well as the area of leaf coverage, a series of CFD simulations to evaluate the air movements within the VGS were performed. This step was undertaken to assess if the plants' porous structure would noticeably enhance the air velocity between the leaf layer and substrate/soil layer, potentially resulting in superior cooling effects due to the critical role of air velocity in evaporative cooling.

The detailed input processes and boundary conditions for the simulation conducted in DesignBuilder are provided in the Methods section. The results (illustrated in Fig. 4.) reveals that, with a porous growth form (VGS 2), the average air velocity through the region between the leaves and growing media layer is approximately 45 % higher as compared to a VGS utilizing plants with a dense growth form (VGS 1). The velocity count in Fig. 4(e) and f. illustrates the frequency of air velocity values in the CFD grids within the segment of the VGS. The figure demonstrated higher occurrence of air-velocity above 0.47 m/s in the porous VGS against the dense VGS. The mean air velocity values of 0.21 m/s and 0.38 m/s within Fig. 4(e) and f. respectively is then utilized in the computation for the estimated rate of evaporation from the growing media and its corresponding evaporative cooling effect.

Equations (1)–(3) (shown in section 3.1) facilitated the computation of evaporation rates and evaporative cooling. Our findings indicate that the porous growth form of VGS 2 could achieve an evaporation rate and cooling effect of up to 0.18 L/m^2/hour and 404.87 kJ/m^2/hour respectively, while the dense growth form of VGS 1 could achieve an evaporation rate and cooling effect of up to 0.15 L/m^2/hour and 338.37 kJ/m^2/hour respectively. This data suggests the porous growth form of VGS 2 produces approximately 16 % higher evaporation and cooling rates compared to VGS 1, whose dense form naturally restricts air velocity in the region between the leaf and growing media layers. However, since these findings are based on a simplified simulation model, we further validated these results through a subsequent experimental study.

4.2. Thermal performance of vertical greenery system over a six-month period

Progressing from the theoretical insights of the CFD simulation evaluation, the exploration then moved towards testing these principles in a real-world experimental setup. The thermal performance of two sets of lightweight VGS substrate panels containing two types of epiphytic plants namely the Philodendron Scandens (VGS 1a) for its dense growth form and Philodendron Burle-Marxii (VGS 2a) for its porous growth form were first compared against a baseline wall with an ETTV value of 48.05 W/m^2. The experiment was also repeated after 6 months when the VGS reached its full growth form, known as VGS 1b and VGS 2b for the full growth form of the Philodendron Scandens (Dense) and Philodendron Burle-Marxii (Porous), respectively. The state of the VGS before and after 6 months can be found in Fig. 5. In addition, at the fully developed state of the VGS panels (after 6 months), spot readings of soil moisture levels of both VGS were recorded at 2pm (2 h after the previous irrigation timing of 12pm), to estimate if the mean soil moisture percentage difference between the 2 panels would be similar to the results found in the CFD evaluation. The soil moisture level is illustrated in Fig. 5 (b) where it shows that the moisture level in VGS 1b is approximately 10 % higher than in VGS 2b. Although the rate is not exactly the same value found in the CFD simulation, 10 % (in the real-world experiment with varying wind speeds) compared to the 16 % (in the CFD simulation with only the predominant wind direction- South to North wind tested), these values still point towards the probable elevated rate of evaporation due to the plant structure of VGS 2b. It is also apparent that the distribution of soil moisture shown in Fig. 5 (b) also corresponds to a similar pattern found in Fig. 4 (c) and (d).

A quantitative summary of the weather station daily average and air-conditioning cooling consumption can be found in Fig. 6. The values in Fig. 6(a) show that the daily solar radiation during the test for VGS 2b was the lowest, followed by VGS 1a, VGS 1b, VGS 2a and Baseline respectively. However, in Fig. 6(b), the outdoor ambient temperatures were highest during the test for VGS 1b, followed by VGS 2b, VGS 2a, Baseline and VGS 1a, respectively. Fig. 6(c) shows the average wind velocity during the test for VGS 2b was the lowest followed by VGS 2a, VGS 1a, VGS 1b and Baseline respectively. Fig. 6(d) then shows an indicative thermal performance of the VGS in reducing the cooling loads in the room. It is apparent that the cooling consumption decreased drastically by approximately 65 % over the baseline after 6 month of plant growth (VGS 1b and 2b). An independent *t*-test was also conducted to check if the weather fluctuations were significantly different between the various iterations of experimental test. The significance test reveals that the weather conditions for Solar radiation, outdoor ambient temperature and windspeeds is not significantly different between each

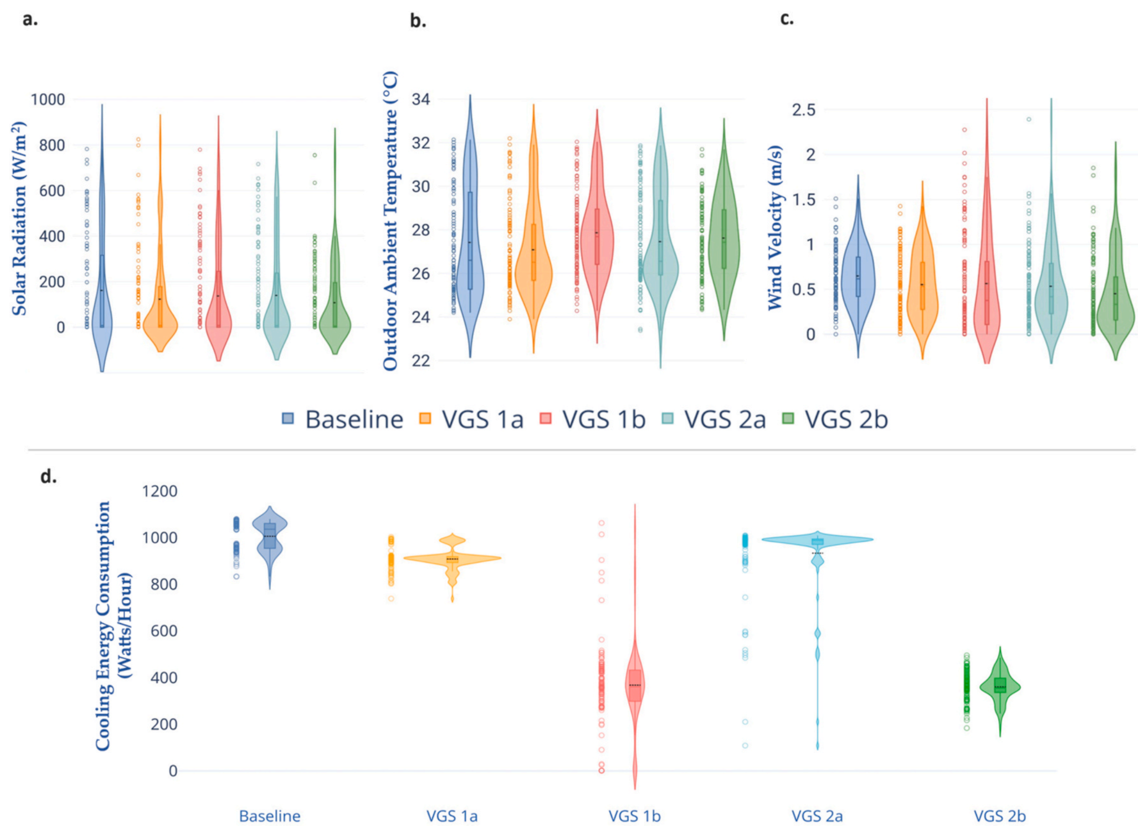

Fig. 6. Weather-Station Daily Average (Top) and Cooling Consumption (Bottom). a, Violin plot of solar radiation during each experimental iteration. **b**, Violin plot of outdoor ambient temperature during each experimental iteration. **c**, Violin plot of wind velocity during each experimental iteration. **d**, Violin plot for cooling energy consumption during each experimental iteration.

iteration namely, Baseline and VGS 1b ($p = 0.338$, $p = 0.899$, $p = 0.799$ respectively), Baseline and VGS 2b ($p = 0.076$, $p = 0.203$, $p = 0.087$ respectively), VGS 1b and VGS 2b ($p = 0.125$, $p = 0.204$, $p = 0.061$ respectively), VGS 1a and VGS 1b ($p = 0.497$, $p = 0.212$, $p = 0.07$ respectively), VGS 2a and VGS 2b ($p = 0.210$, $p = 0.203$, $p = 0.087$ respectively). Therefore, reinforcing that varying weather conditions between each of the experimental iterations would not be a confounder towards the VGS thermal performance.

4.2.1. *Heat flux (façade heat gain)*

Based on the results in Fig. 7(a), it is apparent that VGS 2b performed the best, followed by VGS 1b, VGS 1a and VGS 2a with an average daytime heat flux of -2.32 W/m^2 (120.45 % reduction over baseline), -0.48 W/m^2 (104.21 % reduction over baseline), 3.79 W/m^2 (66.65 % reduction over baseline), 3.87 W/m^2 (65.97 % reduction over baseline) respectively. This is reinforced by the, *t*-test which reveals that the heat flux for VGS 2b is significantly lower than VGS 1b ($p < 0.01$), heat flux for VGS 1b is significantly lower than VGS 1a ($p < 0.01$), heat flux for VGS 2b is significantly lower than VGS 2a ($p < 0.01$), heat flux for VGS 1b is significantly lower than Baseline ($p < 0.01$), heat flux for VGS 2b is significantly lower than Baseline($p < 0.01$).

Normalizing the heat flux with the varying weather conditions between each iteration, a regression and correlation analysis was also conducted. The regression and correlation graphs can be found in Fig. 7. Fig. 7(b) and (c), which normalize the heat flux value of the wall against weather variables such as outdoor ambient temperature and solar radiation, revealed the superior performance of VGS 2b followed by VGS 1b, VGS 1a and VGS 2a respectively, with the baseline wall performing far worse based on the value of the slope and intercept in the regression equation. However, based on the p-value of the correlation coefficient (R), outdoor ambient temperature does significantly affect the heat flux through façade at a 5 % significance level only for Baseline and VGS 2b (Philodendron Burle-Marxii after 6 months). Whereas solar radiation significantly affects the heat flux through the façade at a 5 % significance level only for Baseline, VGS 1a (Philodendron Scandens at the initial stage) and VGS 2b (Philodendron Burle-Marxii after 6 months).

From Fig. 7(b) and (c), it is also apparent that after 6 months of growth, the VGS thermal performance in heat gain reduction has an observable improvement. This is possibly because, with lower leaf coverage and density at the early stages of the VGS, the overall thermal performance was mainly dependent on the VGS lightweight panel construction material and the irrigated soil substrate. However, as the leaf coverage reaches its peak form in about 6 months, it is apparent that it is attributed to the observable improvement to VGS cooling performance after 6 months.

4.2.2. *Outdoor cooling potentials*

The outdoor cooling potentials for each of the VGS were also measured in this experiment and compared to the baseline wall. Based on Fig. 8(a), the temperatures 800 mm in front of the VGS and baseline walls averaged between 27.70 °C and 28.31 °C daily. Based on Fig. 8(b), Normalizing the temperatures 800 mm in front of the walls with the varying ambient outdoor air temperature measured at the weather station, the outdoor cooling potentials of such small scale deployment of VGS did not show sufficient outdoor cooling potentials against the baseline wall, except for VGS 2b and 1b which shows a relatively observable cooling effect over the baseline wall especially at higher outdoor ambient temperatures of around 31 °C, where the temperature at 800 mm away from the wall is approximately 1 °C and 0.5 °C lower than the baseline respectively. Statistical test was also conducted for each of the regression lines shown in Fig. 8(b). The results revealed that the outdoor temperature during all 5 variations significantly affects

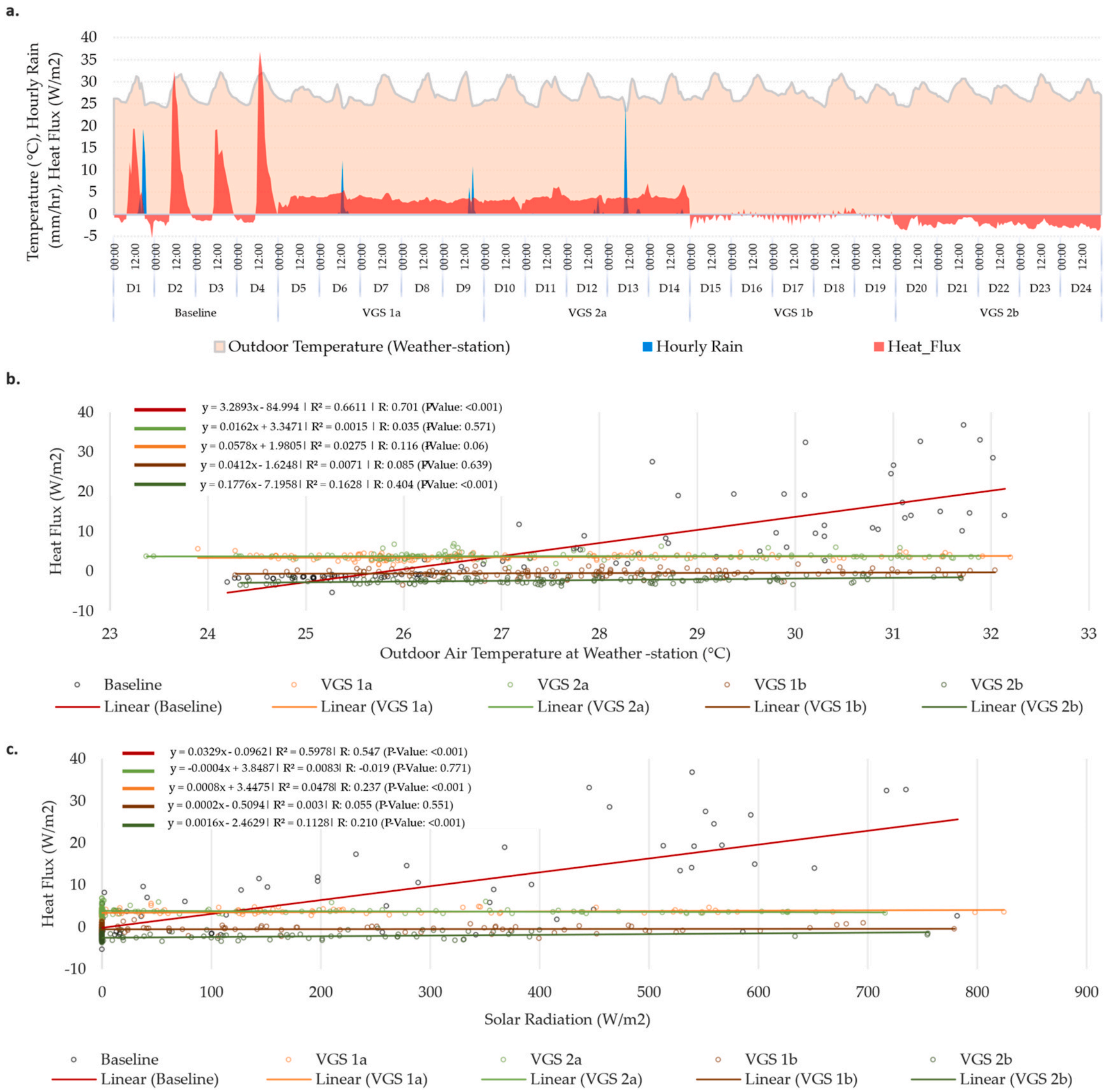

Fig. 7. Heat Flux Through Façade (Raw data and Regression Analysis). a, Timeseries chart of the hourly heat flux and weather conditions. **b**, Regression Analysis of heat flux against the outdoor ambient air temperature. **c**, Regression Analysis of heat flux against the solar radiation data from weather-station.

temperatures 800 mm in front of the wall at a 5 % significance level, with the correlation coefficient of each line ranging between 0.770 and 0.879.

An independent *t*-test was also conducted to find out if any of the VGS provided significant outdoor cooling effects resulting in significantly lower outdoor air temperatures at 800 mm away from the façade. The result of the *t*-test shows that ambient air temperature 800 mm in front of VGS 2b is not significantly lower than VGS 1b ($p = 0.209$), ambient air temperature 800 mm in front of VGS 1b is not significantly lower than VGS 1a ($p = 0.905$), ambient air temperature 800 mm in front of VGS 2b is not significantly lower than VGS 2a ($p = 0.064$), ambient air temperature 800 mm in front of VGS 1b is not significantly lower than Baseline ($p = 0.10$), except for only VGS 2b, where ambient air temperature 800 mm in front of VGS 2b is significantly lower than Baseline ($p = 0.02$).

5. Discussions and limitation

Our CFD simulations, corroborated through experimental setup and soil moisture readings, suggest that an air gap layer between the leaf layer and growing media (by using plants with a porous growth form, providing thick uniform coverage with an air-gap behind the leaves) increases the rate of evaporation from the growing media by up to 16 % (0.03 L/m^2/hour) over a dense VGS growth form, increasing the rate of evaporative cooling by up to 66.5 kJ/m^2/hour. As a result, from the experiments, it was evident that the porous VGS was able to provide a significant outdoor cooling effect of up to 1 °C within 800 mm, and it also results in a negative façade heat flux value of -2.32 W/m^2. This is a significant finding as it may be an essential factor to offset the current limitations of VGS brought about by the phenomenon known as midday stomata closure where plants close their stomata during the hottest parts of the day, thereby inadvertently reducing evapotranspiration and its cooling effect when it's most needed. Instead of relying on just the rate of evapotranspiration of the leaves which are also limited by the midday stomata closure [41], the provision of a porous VGS that also leverages on the evaporative cooling effects of the growing medium enables a sustained thermal performance throughout the day.

From the results of this study, it is also evident that VGS 2b (Full coverage Porous VGS) offers a thermal performance that is notably more effective when compared to VGS 1 (dense) and VGS 2a (Sparse coverage Porous VGS). Most preceding studies have predominantly concentrated on aspects such as leaf coverage or Leaf Area Index (LAI) [23,24]. However, the findings of our investigation propose that leaf coverage is not the sole determinant when assessing the thermal performance of a VGS. We posit that the growth form of the plants on a VGS, influencing the system's porosity, defined here as the provision of space between the

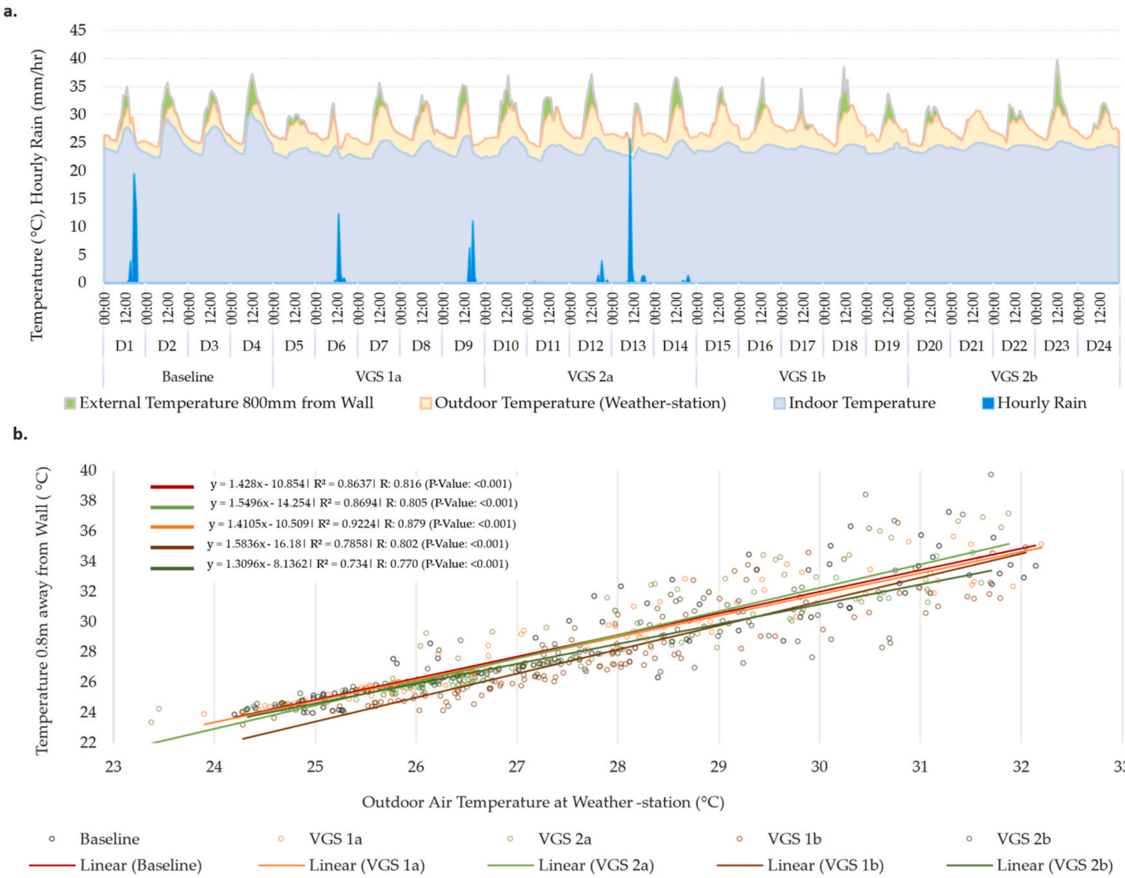

Fig. 8. VGS outdoor cooling (Raw data and Regression Analysis). a, Timeseries chart of the hourly external temperature 800 m from the VGS as well as the outdoor weather parameters. **b**, Regression Analysis of outdoor temperatures 800 mm away from wall against the outdoor ambient air temperature.

leaf layer and the growing media, is another essential factor. This could play a significant role in optimizing the thermal performance of a VGS, extending our understanding of the key elements influencing VGS thermal efficiency.

Additionally, the findings in this study could also be used as a basis for further refining the design of VGS systems, perhaps incorporating meshes or design structures within the VGS panels to enable porosity even when dense plant growth forms are used. This would further enhance and allow for a wider range of biodiversity that could leverage on the thermal performance benefits of a porous VGS. Moreover, the same concept of provisioning for porosity and encouraging the reliance evaporation from the growing media to enhance the cooling effects of greenery could also be considered in related fields such as the field of building integrated photovoltaics (PV), where there have been numerous studies that are looking into the benefits of the co-location of PV with greenery [42]. In a comparison with previous studies conducted at the same location, the Vertical Greenery Systems (VGS) tested in this study clearly outperform established shading strategies. For instance, one of the most optimal daytime shading systems, such as double skin shading [43], exhibits a peak façade heat gain value of 11.31 W/m^2, a reduction of 18.13 W/m^2 (62 %) over the baseline wall. In contrast, the porous VGS from this study shows a strikingly lower peak façade heat gain value of −0.28 W/m^2, translating to a 29.74 W/m^2 (101 %) reduction over the baseline wall. Notably, a key distinction lies in the ability of the porous VGS to consistently maintain within the negative heat gain range. Furthermore, the heat-trapping effect associated with double skin shading, leading to elevated night-time heat gain [43], did not occur when VGS was utilized. This highlights that the cooling effects of VGS is not merely due to the shading effects from the VGS panel. Rather, it is the effect of a complex cooling mechanism within a VGS as illustrated in Fig. 1. Hence, considerations for the complex effects of VGS on the internal building operations such as dynamic optimizations to air-conditioning setpoints and deadbands [44,45], should be addressed in future studies.

Furthermore, this study has its limitations. Firstly, the CFD simulations undertaken were primarily designed as a preliminary investigation to discern the approximate magnitude of wind flowing through the VGS prior to the field experiment. As such, the VGS model in the CFD was considerably simplified, and a uniform free stream wind velocity being used. In addition, parameters such as the walls and component block thermal properties, fluttering movements of leaves and moisture transport and interactions with the air are also not considered in the CFD simulation. Therefore, considerations for these parameters with the effects of plant form porosity in greenery simulations are areas that future studies should look into. Secondly, the field study was conducted only on an East Facing façade, which receives the predominant wind flow direction in the space between the leaf layer and growing media. Therefore, when applied to other facades that do not permit the predominant wind flow direction, the porous VGS may result in a less pronounced thermal performance improvement. Future studies should also aim to address these limitations by investigating the performance of porous VGS on different facades, thereby enhancing the applicability of these findings.

6. Conclusions

Through a multi-faceted study incorporating CFD simulations along with real-world experiments, this paper demonstrated the effect of VGS plant growth form (porous and dense) on air movement within the VGS, a notable factor that has been overlooked in current studies, could notably augment the rate of evapotranspiration and thus its associated cooling effects. This paper offers the following pivotal insights and considerations:

For the first time, this study has demonstrated that a particular plant growth form, which allows for a more substantial air gap between the leaf layer and growing media, can enhance the performance of Vertical Greenery Systems (VGS). With this configuration, it is not only possible for the VGS to provide a significant outdoor cooling effect of up to 1 °C within 800 mm, but it also results in a negative façade heat flux value of -2.32 W/m^2. Specifically, the porous growth form of VGS 2 (Philodendron Burle-Marxii) which has a thick uniform leaf coverage with an air gap, produces superior heat gain reduction and outdoor cooling over VGS 1 (Philodendron Scandens) which has a dense herbaceous vine growth form, by on average 1.84 W/m^2 and 0.5 °C respectively.

The CFD simulation conducted in this study demonstrates a 16 % higher rate of evapotranspiration and evaporative cooling by VGS 2 (porous growth form) over VGS 1 (dense growth form) due to the elevated air velocity that can flow through the spaces between the leaves and growing media. These CFD results were also validated with on-site soil moisture level readings. Therefore, the provision for a layer of ventilation gap between the substrate panel and leaf layer should ideally be considered for, to further enhance the cooling potentials of a VGS. This also shows the importance of a layer of growing media (such as a soil substrate) to hold moisture, enabling a larger surface area for evaporative cooling to occur. In this context, it is notable that evaporation rates attributed to the growing media alone may approximate to 0.15–0.18 L/m^2/hour. Furthermore, by leveraging on the evaporative cooling from the VGS growing media, this study has shown that the provision of a porous VGS enables a sustained thermal performance throughout the day, essentially offsetting the limitations of VGS brought about by midday stomata closure.

This study also revealed the significance of a fully formed (full coverage) VGS in providing the outdoor cooling effect and façade heat gain reduction. Without a complete plant coverage, the VGS largely functions as a regular double skin façade, which falls short of a fully formed VGS's effectiveness. This is potentially the reason why researchers often study the potential cooling effects of greenery systems based on the Leaf Area Index (LAI), as higher LAI would typically mean greater level of leaf shading and rate of evapotranspiration. However, they have overlooked on the fact that the growth structure of the plant does significantly affect the cooling potentials of the VGS as well. The substantial heat gain reduction and outdoor cooling demonstrated by the VGS in this study has also demonstrated that the cooling effects of VGS is not merely due to the shading effects from the VGS panel. Rather, it is the effect of a complex cooling mechanism within a VGS as illustrated in Fig. 1.

CRediT authorship contribution statement

Iqbal Shah: Writing – review & editing, Writing – original draft, Visualization, Validation, Software, Resources, Methodology, Investigation, Formal analysis, Data curation, Conceptualization. **Siu-Kit Lau:** Writing – review & editing, Methodology, Investigation, Data curation, Conceptualization. **Veera Sekaran:** Writing – review & editing, Resources, Methodology, Conceptualization. **Ali Ghahramani:** Writing – review & editing, Writing – original draft, Visualization, Validation, Supervision, Resources, Project administration, Methodology, Investigation, Funding acquisition, Conceptualization.

Declaration of competing interest

The authors declare that they have no known competing financial interests or personal relationships that could have appeared to influence the work reported in this paper.

Data availability

Data will be made available on request.

Acknowledgments

This material is based upon work supported by the Singapore Ministry of Education under grant no A-0008302-02-00 and A-8000136-01-00. Any opinions, findings, and conclusions expressed in this material are those of the authors and do not necessarily reflect the views of the Singapore Ministry of Education.

References

[1] International Energy Agency, The Future of Cooling Opportunities for Energy-Efficient Air Conditioning, IEA, 2018. https://www.iea.org/reports/the-future-of-cooling.
[2] A.R. Katili, R. Boukhanouf, R. Wilson, Space cooling in buildings in hot and humid climates—a review of the effect of humidity on the applicability of existing cooling techniques, in: 14th Int. Conf. Sustain. Energy Technol., 2015, https://doi.org/10.13140/RG.2.1.3011.5287.
[3] W. He, L. Zhang, C. Yuan, Future air temperature projection in high-density tropical cities based on global climate change and urbanization – a study in Singapore, Urban Clim. 42 (2022), 101115, https://doi.org/10.1016/j.uclim.2022.101115.
[4] M. Santamouris, C. Cartalis, A. Synnefa, D. Kolokotsa, On the impact of urban heat island and global warming on the power demand and electricity consumption of buildings—a review, Energy Build. 98 (2015) 119–124, https://doi.org/10.1016/j.enbuild.2014.09.052.
[5] L. Zhang, C. Yuan, Multi-scale climate-sensitive planning framework to mitigate urban heat island effect: a case study in Singapore, Urban Clim. 49 (2023), 101451, https://doi.org/10.1016/j.uclim.2023.101451.
[6] F. Estrada, P. Perron, Disentangling the trend in the warming of urban areas into global and local factors, Ann. N. Y. Acad. Sci. 1504 (2021) 230–246.
[7] D. Zhou, J. Xiao, S. Frolking, L. Zhang, G. Zhou, Urbanization contributes little to global warming but substantially intensifies local and regional land surface warming, Earth's Future 10 (2022), e2021EF002401.
[8] N.H. Wong, C.L. Tan, D.D. Kolokotsa, H. Takebayashi, Greenery as a mitigation and adaptation strategy to urban heat, Nat. Rev. Earth Environ. 2 (2021) 166–181, https://doi.org/10.1038/s43017-020-00129-5.
[9] A.B. Daemei, M. Azmoodeh, Z. Zamani, E.M. Khotbehsara, Experimental and simulation studies on the thermal behavior of vertical greenery system for temperature mitigation in urban spaces, J. Build. Eng. 20 (2018) 277–284.
[10] A.J. Ghazalli, C. Brack, X. Bai, I. Said, Physical and non-physical benefits of vertical greenery systems: a review, J. Urban Technol. 26 (2019) 53–78.
[11] N. Meili, G. Manoli, P. Burlando, J. Carmeliet, W.T.L. Chow, A.M. Coutts, M. Roth, E. Velasco, E.R. Vivoni, S. Fatichi, Tree effects on urban microclimate: diurnal, seasonal, and climatic temperature differences explained by separating radiation, evapotranspiration, and roughness effects, Urban For. Urban Green. 58 (2021), 126970, https://doi.org/10.1016/j.ufug.2020.126970.
[12] A. Beudin, T.S. Kalra, N.K. Ganju, J.C. Warner, Development of a coupled wave-flow-vegetation interaction model, Comput. Geosci. 100 (2017) 76–86, https://doi.org/10.1016/j.cageo.2016.12.010.
[13] B. Gao, J. Farnsworth, K.M. Smits, Evaporation from undulating soil surfaces under turbulent airflow through numerical and experimental approaches, Vadose Zone J. 19 (2020), e20038.
[14] W.-J. Wang, W.-Q. Peng, W.-X. Huai, G.G. Katul, X.-B. Liu, X.-D. Qu, F. Dong, Friction factor for turbulent open channel flow covered by vegetation, Sci. Rep. 9 (2019) 5178, https://doi.org/10.1038/s41598-019-41477-7.
[15] L. Zhang, Z. Deng, L. Liang, Y. Zhang, Q. Meng, J. Wang, M. Santamouris, Thermal behavior of a vertical green facade and its impact on the indoor and outdoor thermal environment, Energy Build. 204 (2019), 109502.
[16] S. Wonorahardjo, I.M. Sutjahja, Y. Mardiyati, H. Andoni, R.A. Achsani, S. Steven, D. Thomas, E. Tunçbilek, M. Arıcı, N. Rahmah, Effect of different building façade systems on thermal comfort and urban heat island phenomenon: an experimental analysis, Build. Environ. 217 (2022), 109063.
[17] J. Peñuelas, J. Pinol, R. Ogaya, I. Filella, Estimation of plant water concentration by the reflectance water index WI (R900/R970), Int. J. Rem. Sens. 18 (1997) 2869–2875.
[18] A. Roman, T. Ursu, Multispectral satellite imagery and airborne laser scanning techniques for the detection of archaeological vegetation marks, Landsc. Archaeol. North. Front. Roman Emp. Porolissum Interdiscip. Res. Proj. Cluj-Napoca Mega Publ. House. (2016) 141–152.
[19] M.F. Shahidan, M.K. Shariff, P. Jones, E. Salleh, A.M. Abdullah, A comparison of Mesua ferrea L. and Hura crepitans L. for shade creation and radiation modification in improving thermal comfort, Landsc. Urban Plann. 97 (2010) 168–181.
[20] H.-Z. Lu, L. Song, W.-Y. Liu, X.-L. Xu, Y.-H. Hu, X.-M. Shi, S. Li, W.-Z. Ma, Y.-F. Chang, Z.-X. Fan, Survival and growth of epiphytic ferns depend on resource sharing, Front. Plant Sci. 7 (2016) 416.
[21] M. Petruzzello, Epiphyte, Encycl. Br. Vol. 1 (2020). https://www.britannica.com/plant/epiphyte.

[22] M. Shahanova, Use and assortment of ornamental epiphytes suitable for vertical gardens in the interior, Forestry 16 (2010) 40.
[23] S.R. Hardwick, R. Toumi, M. Pfeifer, E.C. Turner, R. Nilus, R.M. Ewers, The relationship between leaf area index and microclimate in tropical forest and oil palm plantation: forest disturbance drives changes in microclimate, Agric. For. Meteorol. 201 (2015) 187–195.
[24] K.C. Dahanayake, C.L. Chow, G.L. Hou, Selection of suitable plant species for energy efficient Vertical Greenery Systems (VGS), Energy Proc. 142 (2017) 2473–2478.
[25] A. Abd Ghafar, I. Said, A.M. Fauzi, M. Shariman, Comparison of leaf area index from four plant species on vertical greenery system in Pasir Gudang, Malaysia, Pertanika J Sci Technol 28 (2020) 735–748.
[26] N.H. Wong, A.Y.K. Tan, Y. Chen, K. Sekar, P.Y. Tan, D. Chan, K. Chiang, N. C. Wong, Thermal evaluation of vertical greenery systems for building walls, Build. Environ. 45 (2010) 663–672.
[27] O.H. Dede, N. Mercan, H. Ozer, G. Dede, O. Pekarchuk, B. Mercan, Thermal insulation characteristics of green wall systems using different growing media, Energy Build. 240 (2021), 110872.
[28] T. Safikhani, A.M. Abdullah, D.R. Ossen, M. Baharvand, Thermal impacts of vertical greenery systems, Environ. Clim. Technol. 14 (2014) 5–11.
[29] A.B. Besir, E. Cuce, Green roofs and facades: a comprehensive review, Renew. Sustain. Energy Rev. 82 (2018) 915–939, https://doi.org/10.1016/j.rser.2017.09.106.
[30] B. Jaafar, I. Said, M.H. Rasidi, Evaluating the impact of vertical greenery system on cooling effect on high rise buildings and surroundings: a review, RUAS 9 (2011) 1–9, https://doi.org/10.21776/ub.ruas.2011.009.02.1.
[31] K. Perini, M. Ottelé, E.M. Haas, R. Raiteri, Greening the building envelope, facade greening and living wall systems, Open J. Ecol. 1 (2011) 1–8, https://doi.org/10.4236/oje.2011.11001.
[32] M. Manso, J. Castro-Gomes, Green wall systems: a review of their characteristics, Renew. Sustain. Energy Rev. 41 (2015) 863–871.
[33] C. Yu, W.N. Hien, Thermal impact of strategic landscaping in cities: a review, Adv. Build. Energy Res. 3 (2009) 237–260.
[34] Meteorological Service Singapore, Climate of Singapore, 2023. http://www.weather.gov.sg/climate-climate-of-singapore/.
[35] S. Kuravi, D. Agonafer, Validation of ASHRAE equation to find evaporation rates in humid cavity, in: ASME Int. Mech. Eng. Congr. Expo., 2004, pp. 109–116.
[36] T. Hu, W.Y. Liu, H.D. Wen, L. Song, T.T. Zhang, Q. Chen, S. Liu, Vascular epiphyte populations with higher leaf nutrient concentrations showed weaker resilience to an extreme drought in a montane cloud forest, Plant Biol. 25 (2023) 215–225.
[37] F. Ascione, R.F. De Masi, M. Mastellone, S. Ruggiero, G.P. Vanoli, Green walls, a critical review: knowledge gaps, design parameters, thermal performances and multi-criteria design approaches, Energies 13 (2020) 2296.
[38] D. Tudiwer, A. Korjenic, The effect of living wall systems on the thermal resistance of the façade, Energy Build. 135 (2017) 10–19.
[39] B. Iso, Thermal Insulation—Building Elements—In-Situ Measurement of Thermal Resistance and Thermal Transmittance—Part 1: Heat Flow Meter Method, 2014.
[40] I. Susorova, P. Azimi, B. Stephens, The effects of climbing vegetation on the local microclimate, thermal performance, and air infiltration of four building facade orientations, Build. Environ. 76 (2014) 113–124.
[41] L.M. Aparecido, K. Naylor, I. Werner, R. Braithwaite, E. Schmidt, H. Throop, J. Das, K. Hultine, Cooling Capacity of Urban Trees Exposed to Thermal Stress, AGU Fall Meet. Abstr., 2021, pp. H35X–H1301.
[42] I. Zluwa, U. Pitha, The combination of building greenery and photovoltaic energy production—a discussion of challenges and opportunities in design, Sustainability 13 (2021) 1537.
[43] I. Shah, B. Soh, C. Lim, S.-K. Lau, A. Ghahramani, Thermal transfer and temperature reductions from shading systems on opaque facades: quantifying the impacts of influential factors, Energy Build. 278 (2023), 112604.
[44] R. Talami, I. Dawoodjee, A. Ghahramani, Demystifying energy savings from dynamic temperature setpoints under weather and occupancy variability, Energy Built Environ (2023), https://doi.org/10.1016/j.enbenv.2023.07.001.
[45] A. Ghahramani, K. Zhang, K. Dutta, Z. Yang, B. Becerik-Gerber, Energy savings from temperature setpoints and deadband: quantifying the influence of building and system properties on savings, Appl. Energy 165 (2016) 930–942, https://doi.org/10.1016/j.apenergy.2015.12.115.